Journal of Solid State Chemistry 185 (2012) 18–24

Contents lists available at SciVerse ScienceDirect

Journal of Solid State Chemistry

journal homepage: www.elsevier.com/locate/jssc

Double perovskite $Sr_2FeMoO_{6-x}N_x$ ($x=0.3$, 1.0) oxynitrides with anionic ordering

M. Retuerto [a,b,*], C. de la Calle [a], M.J. Martínez-Lope [a], F. Porcher [c], K. Krezhov [d], N. Menéndez [e], J.A. Alonso [a]

[a] Instituto de Ciencia de Materiales de Madrid, CSIC, Cantoblanco, 28049 Madrid, Spain
[b] Department of Chemistry, Rutgers, State University of New Jersey, Piscataway, NJ 08854-8087, USA
[c] Laboratoire Leon Brillouin, CEA/Saclay, 91191 Gif Sur Ivette Cedex, France
[d] Institute for Nuclear Research and Nuclear Energy, Bulgarian Academy of Sciences, 72 Tsarigradsko Chaussee Boulevard, Sofia 1784, Bulgaria
[e] Departamento de Química Física Aplicada, Facultad de Ciencias, Universidad Autónoma de Madrid, 28049 Madrid, Spain

ARTICLE INFO

Article history:
Received 4 February 2011
Received in revised form
5 October 2011
Accepted 17 October 2011
Available online 25 October 2011

Keywords:
Oxynitride
Perovskite structure
Neutron diffraction
Ammonolysis
Ferrimagnetism

ABSTRACT

Two new oxynitride double perovskites of composition $Sr_2FeMoO_{6-x}N_x$ ($x=0.3$, 1.0) have been synthesized by annealing precursor powders obtained by citrate techniques in flowing ammonia at 750 °C and 650 °C, respectively. The polycrystalline samples have been characterized by chemical analysis, x-ray and neutron diffraction (NPD), Mössbauer spectroscopy and magnetic measurements. They exhibit a tetragonal structure with $a=5.5959(1)$ Å, $c=7.9024(2)$ Å, $V=247.46(2)$ Å^3 for $Sr_2FeMoO_{5.7}N_{0.3}$; and $a=5.6202(2)$ Å, $c=7.9102(4)$ Å, $V=249.85(2)$ Å^3 for Sr_2FeMoO_5N; space group $I4/m$, $Z=2$. The nitridation process seems to extraordinarily improve the long-range Fe/Mo ordering, achieving 95% at moderate temperatures of 750 °C. The analysis of high resolution NPD data, based on the contrast existing between the scattering lengths of O and N, shows that both atoms are located at (O,N)2 anion substructure corresponding to the basal *ab* plane of the perovskite structure, whereas the O1 site is fully occupied by oxygen atoms. The evolution of the ⟨Fe–O⟩ and ⟨Mo–O⟩ distances suggests a shift towards a configuration close to $Fe^{4+}(3d^4, S=2)$:$Mo^{5+}(4d^1, S=1/2)$. The magnetic susceptibility shows a ferrimagnetic transition with a reduced saturation magnetization compared to Sr_2FeMoO_6, due to the different nature of the magnetic double exchange interactions through Fe–N–Mo–N–Fe paths in contrast to the stronger Fe–O–Mo–O–Fe interactions. Also, the effect observed by low-temperature NPD seems to reduce the ordered Fe moments and enhance the Mo moments, in agreement with the evolution of the oxidation states, thus decreasing the saturation magnetization.

1. Introduction

In the last decade, some members of the family of double perovskites of composition $A_2B'B''O_6$ (A=alkali earths, B', B'': transition metals) have been proposed as half-metallic ferromagnets, as an alternative to perovskite manganites [1–3]. At first, Sr_2FeMoO_6 was shown to exhibit intrinsic tunneling-type magnetoresistance at room temperature [1]. In this oxide the B positions of the perovskite structure are occupied alternately by Fe and Mo atoms, in such a way that each FeO_6 octahedron is corner-linked to 6 MoO_6 octahedra, and *vice versa*. The magnetic structure was described [1] as an ordered array of parallel Fe^{3+} ($3d^5$, $S=5/2$) magnetic moments, antiferromagnetically coupled to Mo^{5+} ($4d^1$, $S=1/2$) spins.

Many efforts have been devoted to understand and optimize the properties of Sr_2FeMoO_6, in particular to avoid the effects of the so-called "antisite disorder", implying that some Mo^{5+} cations occupy the positions of Fe^{3+} cations and *vice versa*. It is well known that the intensity of the ferromagnetic interactions decreases when the disorder increases, disturbing the magnetic order temperature (T_C) and the saturation magnetization (M_s) [4–6]. In addition, predictions based upon band-structure calculations suggest that the disorder modifies the band structure of the material by partially suppressing the spin polarization and reducing the half-metallic and ferrimagnetic characteristics of the compound [7,8]. For instance, Niebieskikwiat et al. [9], using solid state methods, obtained a material with $M_S=2.7\ \mu_B$ and $T_C\sim405$ K. Chmaissem et al. [10] also prepared this material by solid state synthesis and subsequently reduction in 1%/99% H_2/Ar flow at high temperatures, describing a compound with 4% of the

* Corresponding author at: Department of Chemistry, Rutgers, State University of New Jersey, Piscataway, NJ 08854-8087, USA.
E-mail address: retuerto@rci.rutgers.edu (M. Retuerto).

0022-4596/$ - see front matter © 2011 Elsevier Inc. All rights reserved.
doi:10.1016/j.jssc.2011.10.026

Fe cations over the Mo positions and $M_S=3.6\ \mu_B$. Martínez et al. [11] and Navarro et al. [12] were able to elaborate Sr_2FeMoO_6 with only 2% of cationic disorder, $M_S=3.75\ \mu_B$ and $T_C\sim420$ K. In a previous work, using wet chemistry methods, we prepared Sr_2FeMoO_6 almost completely ordered with $M_S=3.98\ \mu_B$ and record magnetoresistance at room temperature [2].

Many other double perovskites have been described as possible candidates for half-metallic ferromagnets, for instance A_2FeMoO_6 (A=Ca, Ba) [13,14] or A_2FeReO_6 (A=Ca, Sr, Ba) [15–17] and some other derivatives, obtained by cationic substitution either at A or B sublattices of the perovskite structure. An approach that is much less explored is the replacement of oxygen anions by other suitable elements, such as halogens (F,Cl,…), anfigens (N) or sulfur. In this work we have been able to replace some O by N anions, obtaining the first examples of oxynitride double perovskites.

Transition-metal oxides can be transformed into oxynitrides by ammonolysis, in chemical processes in which ammonia behaves as a nitriding agent and additionally induces a change in the oxidation state of the involved transition metals. The increase in the covalency of the crystal structure induced by this replacement at the anion substructure many times brings about an electron delocalization effect, although yielding more insulating materials as a consequence of the strong perturbation of the periodic potential at the anion substructure [18]. From the structural point of view, oxynitrides often show the same structural type as the parent oxides for moderate substitutional rates [19]. The lower oxidizing power of nitrogen as compared to oxygen, leads to the difficulty of forming completely nitrided perovskites (ABN_3) or pyrochlores ($A_2B_2N_7$): oxynitrides with partial nitrogen content are preferentially obtained [19,20].

The precise location of the nitrogen atoms and their role in the structural arrangement of oxynitrides can be investigated by neutron diffraction, as the x-ray scattering factors of oxygen and nitrogen are not sufficiently different to permit the two atoms to be distinguished. Among the oxynitrides studied by neutron diffraction, most of them exhibit a random distribution of O and N over the anion sublattice, as observed for the pyrochlore $Y_2Mo_2O_{4.5}N_{2.5}$ [19]. Only a few oxynitrides are shown to exhibit an ordered nitrogen/oxygen arrangement: this is the case, for instance, of TaON [21] with ZrO_2 baddeleyite structure, or Nd_2AlO_3N [22], Sr_2TaO_3N [23] with K_2NiF_4-type structure and $SrMO_2N$ (M=Nb, Ta) [24] with perovskite structure.

In this work we have prepared partially nitrided derivatives of the Sr_2FeMoO_6 double perovskite, showing ordering at the O/N anion sublattice, nitride ions only occurring at the basal *ab* plane of the perovskite. These materials were obtained by ammonolysis of precursor powders annealed at selected temperatures under a NH_3 gas flow and its characterization was performed by x-ray and neutron powder diffraction (NPD), chemical analysis, Mössbauer spectroscopy and magnetic measurements.

2. Experimental

The samples were prepared in a two-step procedure. Precursor powders were synthesized by a soft-chemistry citrate route. This technique has the advantage to produce homogeneous and reactive precursor oxides and at moderate synthesis temperatures. Stochiometric amounts of $Sr(NO_3)_2$, $FeC_2O_4\cdot2H_2O$ and $(NH_4)_6Mo_7O_{24}\cdot4H_2O$ were dissolved in citric acid. The citrate and nitrate solutions were slowly evaporated leading to organic resins that contain a homogeneous distribution of the involved cations. The resins were dried and annealed at increasing temperatures, with a final treatment in air at 800 °C for 2 h. The second step consists of the ammonolysis of the precursor oxides. The powders were placed in alumina boats and treated in a tube furnace under an ammonia flow (Alpha Gaz N36 B10 ppm $H_2O<400$) of 0.12 l min^{-1} at 650 °C and 750 °C for 6 h.

The N content of the samples was measured in a PE 2400 Series II CSNS/O Analyzer from Perkin Elmer. Acetanilide was used as calibration standard for nitrogen.

The characterization and phase purity of the starting precursors and resulting products were studied by x-ray powder diffraction (XRPD) using a Bruker-axs D8 diffractometer (40 kV, 30 mA), controlled by a DIFFRACT^{plus} software, in Bragg–Brentano reflection geometry with Cu$K\alpha$ radiation ($\lambda=1.5418$ Å) and PSD detector. The data were obtained between 10° and 65° 2θ in steps of 0.05°. Neutron powder diffraction (NPD) diagrams were collected at the Laboratory Leon–Brillouin, Saclay (France) at 295 K and 2 K at the 3T2 diffractometer with a $\lambda=1.2267$ Å wavelength. The refinement of the crystal structure was performed by the Rietveld method [25], using the WinPLOTR [26,27] application and the FULLPROF refinement program [28]. A Thomson–Cox–Hastings pseudo-Voigt convoluted with axial divergence asymmetry function was chosen to generate the line shape of the diffraction peaks [29–31]. The coherent scattering lengths for Sr, Fe, Mo, O and N were: 7.020, 9.450, 6.715, 5.803 and 9.360 fm, respectively.

A Mössbauer spectrum was recorder in triangle mode using a conventional spectrometer with a ^{57}Co/Rh source. The analysis of the spectra was made by nonlinear fit using the NORMOS program [32], and the energy calibration was made with an α-Fe (6 μm) foil.

The *dc*-magnetic susceptibility was measured with a SQUID commercial superconducting quantum interference device on powder samples, in the temperature range of 5–400 K. Magnetization isotherms were measured at selected temperatures in the magnetic field range from −5 T to +5 T.

3. Results and discussion

Two samples of $Sr_2FeMoO_{6-x}N_x$ oxynitrides were obtained as black polycrystalline powders after thermal treatment of the precursor powders at 650 °C and 750 °C in a NH_3 flow. For the sample treated at 650 °C the chemical analysis yields a N contents (x) of 1.00(5), whereas for the 750 °C sample $x=0.30(5)$. The laboratory XRD diagrams at room temperature (RT) of the starting precursor and both oxynitride perovskites are shown in Fig. 1a, b, and c, respectively. A pure ordered Sr_2FeMoO_6 perovskite is also shown in Fig. 1d for the sake of comparison. This last material requires thermal treatments up to 1200 °C in a H_2(1%)/Ar(99%) reducing flow to reach an almost complete Fe/Mo long range ordering [2].

In the three cases the perovskite structure exhibits a tetragonal symmetry; the unit-cell parameters are $a=5.6202(2)$ Å and $c=7.9102(4)$ Å, $V=249.85(2)$ Å^3 for Sr_2FeMoO_5N; $a=5.5959(1)$, $c=7.9024(2)$ Å, $V=247.46(2)$ Å^3 for $Sr_2FeMoO_{5.7}N_{0.3}$ and, as a reference, 5.5690(5), 7.8994(9) Å, 244.99(1) Å^3 for the almost fully ordered Sr_2FeMoO_6 sample obtained at 1200 °C [2]. In Fig. 1d the ordered Sr_2FeMoO_6 perovskite shows superstructure peaks arising from the Fe/Mo ordering (e.g., 001 and 013 reflections). These superstructure peaks are visible, at the same angles, for $Sr_2FeMoO_{5.7}N_{0.3}$, but are much weaker for the Sr_2FeMoO_5N compound, exhibiting a poorer crystallinity. The XRD pattern of the $x=1$ compound suggests, thus, the formation of a pure, partially disordered double perovskite oxynitride. From the analysis of the intensities of these reflections, via Rietveld refinements from the XRD data, the degree of ordering was estimated to be of 95% and 78% for $x=0.3$ and $x=1.0$ samples, respectively. The Rietveld plots are illustrated in Fig. 2. If we define the parameter

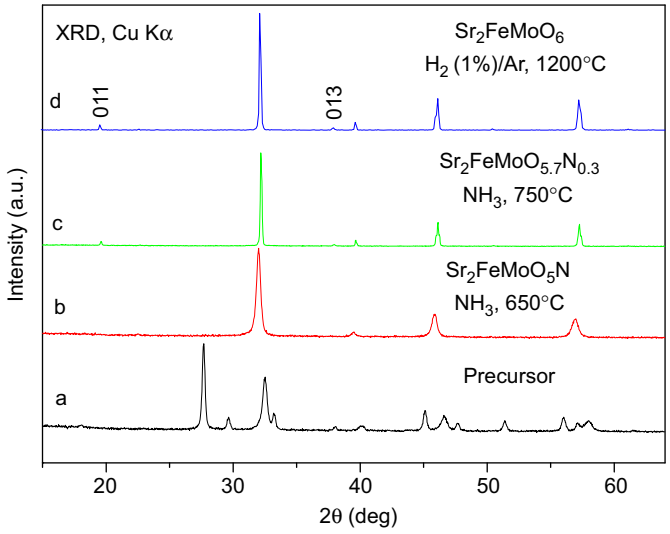

Fig. 1. XRD patterns for (a) the precursor powder, annealed in air at 800 °C, (b) Sr_2FeMoO_5N perovskite, treated at 650 °C in NH_3 flow, (c) $Sr_2FeMoO_{5.7}N_{0.3}$, annealed in NH_3 at 750 °C and (d) pristine Sr_2FeMoO_6, annealed in H_2(1%)/Ar(99%) at 1200 °C.

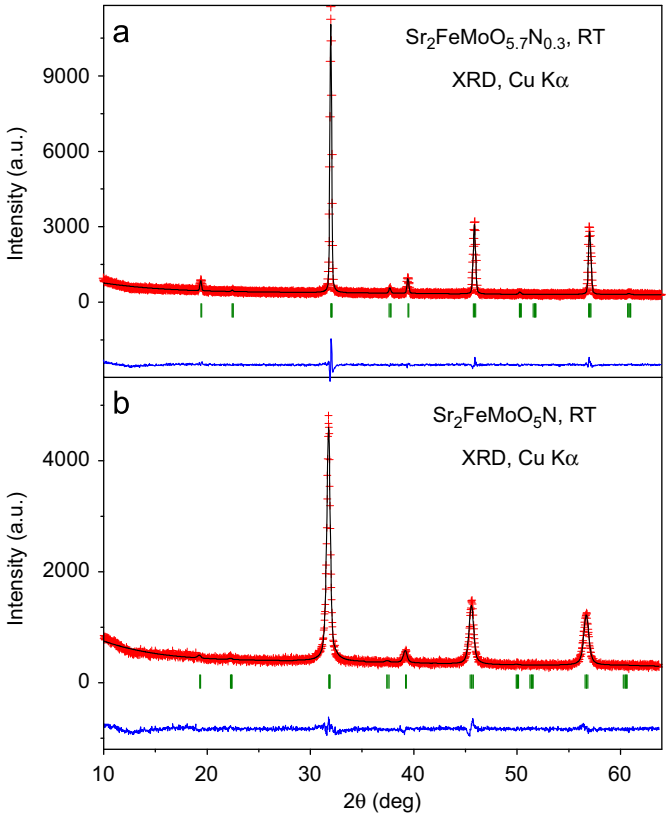

Fig. 2. Observed (crosses), calculated (full line) and difference (bottom) Rietveld profiles for (a) $Sr_2FeMoO_{5.7}N_{0.3}$ and (b) Sr_2FeMoO_5N at 295 K from XRD data.

asd as the fraction of Mo atoms at Fe positions, we have *asd*=0.22 for the $x=1.0$ sample. Notice that *asd* would take a value of 0.5 for a completely disordered sample. It is remarkable that the $x=0.3$ sample exhibits an Fe/Mo long-range ordering as high as 95% (*asd*=0.05) even if it has been annealed at temperatures as low as 750 °C; as a reference the almost fully ordered Sr_2FeMoO_6 double perovskite with record T_C and M_S [2] had to be annealed at 1200 °C (in 1% H_2 flow) in order to minimize the antisite-disordering, with *asd*=0.06. It seems that annealing in NH_3 has a beneficial effect concerning the optimization of the Fe/Mo long-range ordering although, as we will describe later, the magnetic properties become hindered upon N insertion into the anion sublattice.

It is worth mentioning that the ammonolysis of a previously obtained Sr_2FeMoO_6 ordered double perovskite (that shown in Fig. 1d) did not lead to the wanted incorporation of N into the anionic sublattice. It seems essential to start from very reactive precursors (previously treated in air up to 800 °C only) to consolidate a mixed-anion network. In order to understand the different results obtained after the treatments at 650 and 750 °C, it is pertinent to consider the nature of the reactions between the precursor oxides and ammonia. It is well known that NH_3 can act both as a nitriding and a reducing agent: when NH_3 acts as a reducing agent, the solid product is accompanied by a loss of water and nitrogen molecules as byproducts; during the nitridation the formed oxynitride is accompanied by water and hydrogen molecules. In addition, at temperatures above 300 °C ammonia undergoes considerable dissociation: $2NH_3 \leftrightarrow N_{2(g)}+3H_{2(g)}$. The formed hydrogen can also reduce the precursor oxides. Depending on the relative rates of the processes described, a more nitrided or more reduced product can be formed. To achieve the most effective nitridation conditions, the ammonia dissociation process should be minimized before it reaches the sample's surface [33]; if not, the reduction may overcome the nitridation. Consequently, an increase of the ammonia flow with the temperature is essential. Thus, increasing the ammonia flow promotes water removal and the regeneration of active nitriding species on the sample's surface [34,35]. The partial dissociation of the ammonia at elevated temperatures (i.e. 750 °C) before reaching the surface of the material accounts for the stabilization of an oxynitride phase with a low content of nitrogen ($x=0.3$). The nitrogen content could be optimized at lower treatment temperatures (650 °C), although as a drawback a poorer crystallinity of the perovskite sample was observed.

A progressive expansion of the unit cell is observed upon N introduction, as a result of the bigger ionic size of N^{3-} (1.46 Å in fourfold coordination) *vs* O^{2-} (1.38 Å) [36]. Whereas the main reflections of the precursor powder (Fig. 1a) can be identified as a mixture of $SrMoO_4$ with sheelite structure and $SrFeO_{3-\delta}$ perovskite, the obtained nitrided phases are free of sheelite phase. Apparently, the nitridation process is favorable for the stability of the perovskite structure. In a prototypical example, the comparison of the tolerance factors of ABO_3 compared to those of the corresponding oxynitrides in (Ca,Sr,Ba)MoO_3 perovskites upon partial replacement of O^{2-} with N^{3-}, led to conclude that the nitridation reduces the structure distortion energy. By contrast, $AMoO_4$ sheelite phases decompose to AO and MoO_2 when reacted with flowing ammonia [37].

A NPD study was useful to investigate the structural details of Sr_2FeMoO_5N. This sample was selected, in spite of its lower crystallinity, because of its optimized N contents. Two patterns were collected, at 295 K (RT) and 2 K. The crystal structure was defined in the *I*4/*m* space group (No. 87) $Z=2$, with unit cell parameters related to a_0 (ideal cubic perovskite, $a_0 \approx 3.9$ Å) as $a=b \approx \sqrt{2}a_0$, $c \approx 2a_0$; in the present case $a=5.6202(2)$ Å and $c=7.9102(4)$ Å. Sr atoms were located at 4*d* (0, ½, ¼) positions, Fe at 2*a* (0, 0, 0), Mo at 2*b* (0, 0, ½) sites, oxygen atoms O1 at 4*e* (0, 0, *z*) and O2 at 8*h* (*x*, *y*, 0). The anti-site disordering obtained from the XRD pattern (22%) was included in the model, but it was not refined since a strong correlation with the magnetic contribution to the scattering was found in trial refinements. The inclusion of N atoms distributed at random with O1 and O2 resulted in rejection from the O1 sites and convergence to the mixed (O,N)2 occupancy factors included in Table 1, together with the unit-cell, atomic, displacement parameters and discrepancy factors after the refinement at RT and 2 K. The refined occupancy for N is slightly lower

Table 1
Structural parameters for Sr_2FeMoO_5N phase after the Rietveld refinement from NPD data at 295 K and 2 K in the tetragonal $I4/m$ space group; $Z=2$. Reliability factors are also given.

T (K)	295	2
a (Å)	5.6202(2)	5.6117(2)
c (Å)	7.9102(4)	7.8949(4)
V (Å^3)	249.85(2)	248.62(2)
Sr 4*d* (0, 1/2, 1/4)		
B (Å^2)	1.58(4)	1.24(4)
Fe 2*a* (0, 0, 0)		
B (Å^2)	0.9(4)	2.3(2)
$m(\mu_B)$	1.09(7)	2.2(1)
Occ (Fe/Mo)$_{2a}$[a]	0.781(8)/0.219(8)	0.781(8)/0.219(8)
Mo 2*b* (0, 0, 1/2)		
B (Å^2)	2.0(5)	1.7(4)
$m(\mu_B)$	−1.09(7)	−1.2(1)
Occ (Mo/Fe)$_{2b}$[a]	0.781(8)/0.219(8)	0.781(8)/0.219(8)
O1 4*e* (0, 0, *z*)		
z	0.2553(4)	0.2444(3)
B (Å^2)	1.4(2)	1.3(2)
Occ	0.98(5)	0.98(5)
(O/N)2 8*h* (*x*, *y*, 0)		
x	0.2506(3)	0.2567(2)
y	0.2438(3)	0.2363(2)
B (Å^2)	1.6(1)	1.4(1)
Occ (O/N)	0.77(1)/0.23(1)	0.77(1)/0.23(1)
Reliability factors		
χ^2	2.76	3.37
R_p (%)	2.62	2.75
R_{wp} (%)	3.40	3.60
R_{exp} (%)	2.04	1.96
R_{Bragg} (%)	4.00	5.94
R_{mag} (%)	16.7	10.0

[a] The Fe/Mo occupancy factors were determined from XRD data and fixed in the refinement of the NPD data.

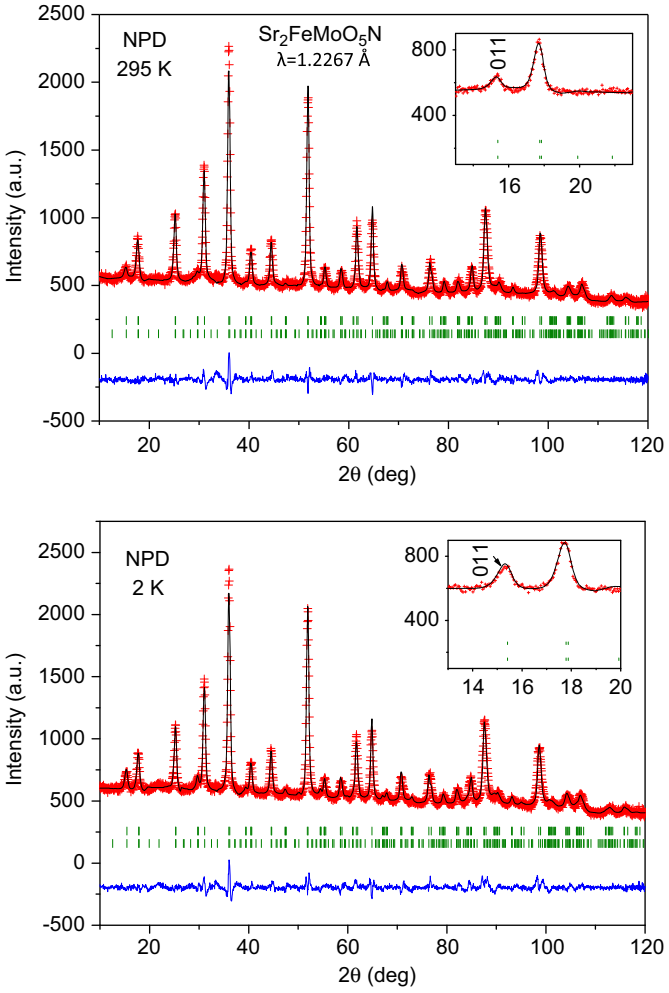

Fig. 3. Observed (crosses), calculated (full line) and difference (bottom) NPD Rietveld profiles for Sr_2FeMoO_5N at 295 K and 2 K. The two series of tick marks correspond to the allowed Bragg reflections for the main phase and the magnetic structure. The inset highlights the first reflections where a magnetic contribution to the scattering is observed.

Table 2
Main interatomic distances for Sr_2FeMoO_5N at 295 K and 2 K.

T (K)	295	2
$(Fe/Mo)_{2a}O_6$ octahedra		
$(Fe/Mo)_{2a}$–O1 (*x*2)	1.940(3)	1.930(2) (*x*2)
$(Fe/Mo)_{2a}$–(O,N)2 (*x*4)	1.965(2)	1.9579(14) (*x*4)
$\langle(Fe/Mo)_{2a}$–(O,N)$\rangle$	1.953	1.944
$(Mo/Fe)_{2b}O_6$ octahedra		
$(Mo/Fe)_{2b}$–O1 (*x*2)	2.015(3)	2.018(2)
$(Mo/Fe)_{2b}$–(O,N)2 (*x*4)	2.010(2)	2.0134(15)
$\langle(Mo/Fe)_{2b}$–(O,N)$\rangle$	2.013	2.016
$(Fe/Mo)_{2a}$–O1–$(Mo/Fe)_{2b}$	180.0	180.0
$(Fe/Mo)_{2a}$–(O,N)2–$(Mo/Fe)_{2b}$	178.44(8)	175.33(6)

than expected, 0.91(4) atoms per formula unit. The occupancy of O1 is stoichiometric within the e.s.d.s. It seems that N is only present at the basal *ab* plane of the perovskite structure. This is concomitant with the flattened character of the tetragonal subcell or aristotype, where $a_0=3.974$ Å and $c_0=3.955$ Å at RT, $c_0/a_0=0.995$, whereas in the canonical Sr_2FeMoO_6 double perovskite the tetragonal substructure is elongated, $a_0=3.938$ Å, $c_0=3.950$ Å, $c/a=1.003$ [2].

Fig. 3 shows the Rietveld fits for the two temperatures. A significant magnetic scattering on the low angle reflections for both 295 K and 2 K diagrams was observed, with a reinforced magnetic contribution on the 011 reflection at 2 K (see insets of Fig. 3). A global ferrimagnetic structure (magnetic moments at the Mo position in an AFM arrangement with respect to the moment over Fe position) was modeled in both cases; after the final refinement, ordered moments of 2.2(1) μB and −1.2(1) μB were obtained for Fe and Mo positions, respectively, at 2 K, and 1.1(1) and −1.1(1) μB at 295 K, in a virtually AFM collinear structure.

Table 2 shows the main interatomic distances and angles for the sample at RT and 2 K; Fig. 4 illustrates a projection along *c* of the tetragonal crystal structure. It consists of a three-dimensional arrangement of FeO_5N and MoO_5N octahedra sharing vertices; in each octahedron, one out of four ions in the basal plane are nitride ions, whereas the two apical ones are always oxide ions. The structure can be described as the result of a single anti-phase octahedral tilting along the *c*-axis. The magnitude of this tilting can be simply derived from the Fe–(O,N)2–Mo angle as

$$\phi = \frac{180 - \langle \mathrm{Fe}-(\mathrm{O,N})2-\mathrm{Mo}\rangle}{2}$$

This angle evolves from a maximum value of $\phi=2.33(6)^\circ$ at 2 K to $\phi=1.56(8)^\circ$ at 295 K.

The FeO_6 and MoO_6 octahedra present a slight axial distortion (compressed and elongated along the *c* axis, respectively). The average $\langle$ Fe–O $\rangle$ and $\langle$ Mo–O $\rangle$ bond lengths, of 1.953 and 2.013 Å at RT, are considerably different from those given by Retuerto

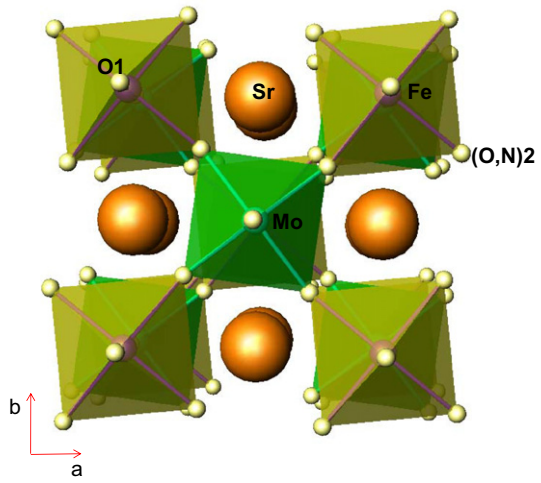

Fig. 4. Schematic representation of the crystal structure of Sr_2FeMoO_5N, approximately projected along the [001] direction, showing the antiphase tilting of the $Fe(O,N)_6$ and $Mo(O,N)_6$ octahedra.

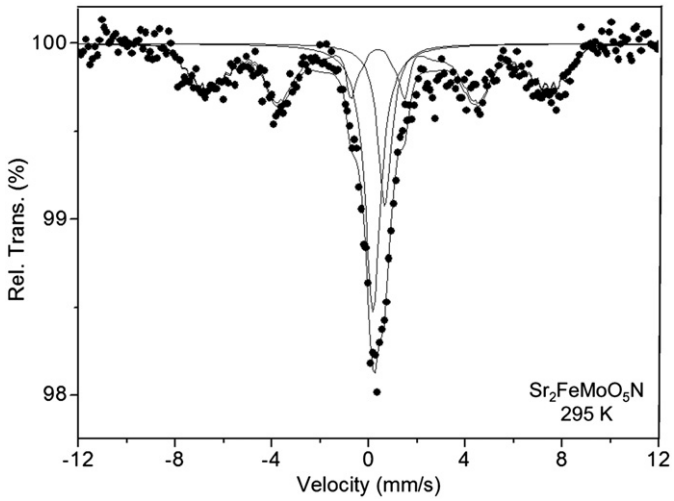

Fig. 5. Mössbauer spectrum of Sr_2FeMoO_5N, collected at 295 K, showing a sextuplet corresponding to the antiferromagnetic ordering exhibited at this temperature. It is fitted to tree contributions (see text).

et al. [2] for a well-crystallized, perfectly ordered Sr_2FeMoO_6 sample, of 2.003 and 1.947 Å, respectively; surprisingly the $\langle$Fe–(O,N)$\rangle$ distances in Sr_2FeMoO_5N are considerably smaller than the $\langle$Mo–(O,N)$\rangle$ distances, in contrast to that observed in the canonical Sr_2FeMoO_6 double perovskite. When the anti-site disordering increases in this oxide, both kinds of octahedra tend to exhibit equal sizes, for instance of 1.97(5) and 1.98(5) Å, respectively, at 15 K [5], since a complete disordering tends to homogenize B'–O and B''–O distances. However it has never been observed that the Fe coordination polyhedron becomes smaller. This observation gives an important clue about the electronic rearrangement of the transition metals upon nitridation: it seems that Fe is becoming strongly oxidized as N^{3-} is incorporated into the crystal structure, whereas Mo–O distances appear to be longer due the larger size of N^{3-} *vs* O^{2-} ions. If we start from a nominal electronic configuration $Fe^{2.5+}$:$Mo^{5.5+}$ for Sr_2FeMoO_6, as it is commonly accepted, we conceive that we are shifting towards a configuration $Fe^{4+}(3d^4, S=2)$:$Mo^{5+}(4d^2, S=1)$. In the ionic limit, we propose a stoichiometry close to $Sr_2Fe^{4+}Mo^{5+}O_5N$ for the $x=1$ compound. We are, thus, reinforcing the magnetic moments at the Mo sites and reducing the spin of Fe ions. This accounts for the evolution of the ordered spins refined in the magnetic structure at 2 K, of 2.2(1) μ_B and −1.2(1) μ_B for Fe and Mo, respectively (Table 1), reduced and enhanced, respectively, regarding to those found in Sr_2FeMoO_6, of 3.9 μ_B and −0.37 μ_B, respectively, at 15 K [5]. It could seem surprising that Fe^{4+} may be stabilized in a reducing environment such as the NH_3 flow. However, the nitriding effect, introducing N^{3-} in the anion sublattice is shown to overcome the reducing effect of NH_3 and thus to stabilize transition metals in high oxidation states; for instance $Mo^{5.5+}$ is stabilized in $Y_2Mo_2O_{4.5}N_{2.5}$ from $Y_2Mo_2O_7$ (Mo^{4+}) [19], or $SrNbO_2N$, containing Nb^{5+}, is stabilized at 1000 °C in NH_3 flow [24].

In order to confirm the presence of Fe in a high oxidation state, a Mössbauer spectrum was collected at room temperature for the $x=1$ sample, shown in Fig. 5. The spectrum fitting was obtained taking into account three contributions. The most abundant component (51% of the resonant area) is a magnetic hyperfine field distribution, which mean hyperfine parameters are $\delta=0.37$ mm/s and $B_{hf}=41$ T, characteristic of antiferromagnetically ordered Fe^{3+} as observed into the double perovskite Sr_2FeMoO_6. Overlapped to this subspectrum there are two broad single lines with $\delta=0.66$ mm/s and $\delta=0.16$ mm/s, respectively. A single line with isomer shift of 0.66 mm/s is in agreement with the reported values for Fe with valence between +2 and +3 in these systems. The third component, 32% of the resonant area, corresponds to more oxidized Fe, therefore the presence of Fe^{+4} could be supported by Mössbauer spectroscopy. To confirm this assignment we have also tried to study the sample above T_N, but unfortunately, the sample decomposed upon heating above 300 °C under the vacuum conditions of the furnace.

The *dc* magnetic susceptibility for $Sr_2FeMoO_{5.7}N_{0.3}$ (Fig. 6a) and Sr_2FeMoO_5N (Fig. 7a) samples exhibit a spontaneous increase of the magnetization upon cooling, characteristic of ferromagnets. For the sample with N contents $x=0.3$ (Fig. 6a), the T_C is above 400 K. For this weak degree of nitridation we still observe similar properties (but with smaller magnetization values) to those observed for the pristine Sr_2FeMoO_6 oxide (inset Fig. 6a and b), where a T_C of 410 [2] or even 430 K [36] has been reported. Sr_2FeMoO_5N oxynitride presents a broad transition that does not reach saturation even at very low temperatures (Fig. 7a). T_C is difficult to estimate due to the broadness of the magnetic transition from paramagnetic to ferromagnetic; it should be in the 150–200 K temperature range. Above 400 K it is expected to exist a second anomaly in the susceptibility since the NPD data at RT already show an AFM ordering with a non-negligible ordered moment at both Fe and Mo sites of 1.1(1) μ_B. We can define, thus, two magnetic ordering temperatures; a T_N establishing the onset for AFM interactions, well above RT, and a T_C, corresponding to the ferrimagnetic interactions, in the 150–200 K range.

From the magnetization *vs* magnetic field isotherms represented in Figs. 6b and 7b we obtain a saturation magnetization of $M_s=0.90$ μ_B/f.u. for the $x=0.3$ oxynitride, and $M_S \approx 0.35$ μ_B/f.u. for the $x=1$ perovskite at 5 K. For $Sr_2FeMoO_{5.7}N_{0.3}$ the magnetization curve (Fig. 6b) is characteristic of a ferrimagnetic systems, with a saturation magnetization well below the expected 4 μ_B for a perfect Fe^{3+} $(3d^5, S=5/2)-Mo^{5+}$ $(4d^1, S=1/2)$ ferrimagnetic system, which could be accounted for the different nature of the magnetic double exchange interactions through Fe–N–Mo–N–Fe paths compared with the better known Fe–O–Mo–O–Fe interactions. It is certainly surprising that this almost fully Fe/Mo ordered double perovskite presents such a low M_s; the presence of 0.3 N^{3-} ions per formula unit is enough to produce a strong perturbation of the periodic potential at the anion substructure and to strongly disturb the double exchange paths, hindering the establishment of a perfect ferrimagnetic arrangement between Fe and Mo spins. Also, the effect observed by NPD seems to reduce

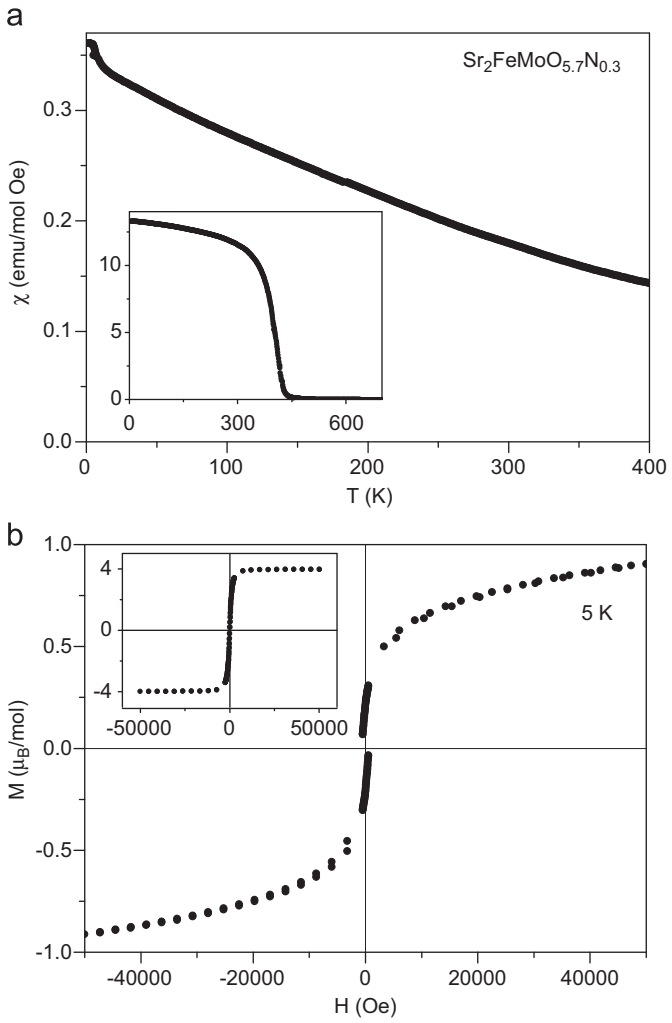

Fig. 6. (a) Temperature variation of the magnetic susceptibility for $Sr_2FeMoO_{5.7}N_{0.3}$, the inset shows the curve for Sr_2FeMoO_6 and (b) isothermal magnetization *vs* magnetic field cycle for $Sr_2FeMoO_{5.7}N_{0.3}$ at $T=5$ K, the inset shows the isothermal curve for Sr_2FeMoO_6.

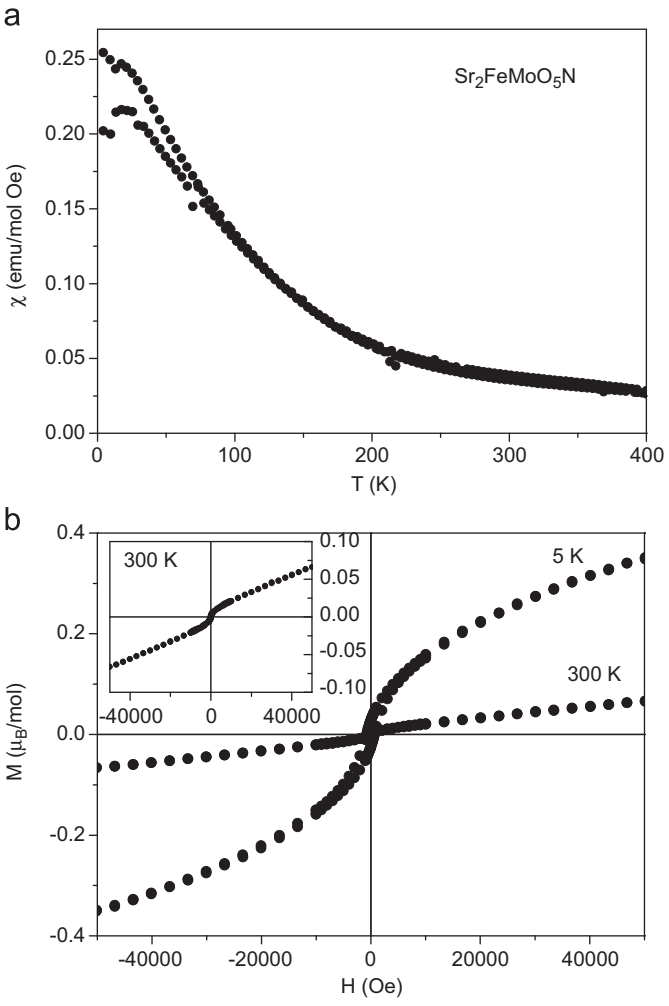

Fig. 7. (a) Temperature variation of the magnetic susceptibility for Sr_2FeMoO_5N recorded with zero-field cooled (ZFC) and field cooled (FC) conditions and (b) isothermal magnetization *vs* magnetic field isotherms for $T=5$ K and 300 K.

the Fe moments and increase the Mo moments, thus reducing the saturation magnetization. As for the $x=1$ oxynitride, an additional reduction of M_s comes from a certain degree of antisite disordering, implying that some Fe occupy the Mo sites and *vice versa*, giving rise to the existence of Fe-rich patches, naturally occurring in disordered samples and responsible for a pure antiferromagnetic arrangement of the neighboring Fe magnetic moments [17,38,39]. It is noteworthy that the 300 K isotherm (Fig. 7b) corresponds to an antiferromagnetic material, showing no curvature indicating a perfectly compensated B' and B'' sublattices; the presence of magnetic scattering coming from this AFM structure suggests a Néel ordering temperature above 400 K, as observed in Sr_2FeMoO_6 systems with a high level of antisite disordering, where T_N's of 750 K have been reported [5].

4. Conclusions

Two oxynitride double perovskites are reported for the first time, of composition $Sr_2FeMoO_{5.7}N_{0.3}$ and Sr_2FeMoO_5N (determined by chemical analysis). They have been prepared by ammonolysis of precursor powders of Sr_2FeMoO_6 stoichiometry. Both samples are tetragonal and the unit-cell volumes are noticeably expanded with respect to the pristine compound, due to the bigger size of N^{3-} *vs* O^{2-}. Annealing in NH_3 flow seems to favor the long-range ordering of Fe and Mo ions over the B' and B'' sites of the double perovskite, obtaining an almost fully ordered perovskite (95%) at moderate temperatures of 750 °C. As determined by a NPD study of a selected sample, N atoms are preferentially found at the basal *ab* plane of the perovskite structure, which is in connection with the flattened tetragonal subcell; surprisingly the average ⟨Fe–O⟩ distances are extremely reduced with respect to those found in the canonical Sr_2FeMoO_6 double perovskite, suggesting an oxidation effect due to the introduction of N^{3-} anions, whereas ⟨Mo–O⟩ bond-lengths substantially increase, indicating a redistribution of the electronic density, towards a configuration close to $Fe^{4+}(3d^4, S=2)$:$Mo^{5+}(4d^1, S=1)$; a Moessbauer spectrum collected at RT is compatible with the presence of Fe^{4+}. The magnetic properties undergo a strong modification upon N introduction; the long-range ferrimagnetic ordering characteristic of Sr_2FeMoO_6 becomes hindered, with a substantial decrease of the saturation magnetization and T_C for the more heavily substituted compound: the ordered magnetic moment on the Fe sites tends to decrease whereas that of Mo increases as a consequence of the mentioned electronic redistribution induced upon nitridation.

Acknowledgments

We acknowledge the financial support of the Spanish Ministry of Education to the project MAT2010-16404, and the Fulbright

Commission for the grant of Dr. M. Retuerto. We are grateful to Dr. M. García-Hernández for performing the magnetic measurements. We thank the LLB, Saclay, France for making the neutron beam time available. We are also grateful for the CSIC-BAS project P2007BG0013.

References

[1] K.I. Kobayashi, T. Kimura, H. Sawada, K. Terakura, Y. Tokura, Nature 395 (1998) 677–680.
[2] M. Retuerto, J.A. Alonso, M.J. Martínez-Lope, J.L. Martínez, M. García-Hernández, Appl. Phys. Lett. 85 (2004) 266–268.
[3] M. Retuerto, J.A. Alonso, M.J. Martínez-Lope, N. Menéndez, J. Tornero, M. García-Hernández, J. Mater. Chem. 16 (2006) 865–873.
[4] J. Navarro, J. Nogues, J.S. Muñoz, J. Fontcuberta, Phys. Rev. B. 67 (2003) 174416.
[5] D. Sanchez, J.A. Alonso, M. García-Hernández, M.J. Martinez-Lope, J.L. Martínez, Phys. Rev. B. 65 (2002) 104426–104428.
[6] L. Balcells, J. Navarro, M. Bibes, A. Roig, B. Martínez, J. Fontcuberta, Appl. Phys. Lett. 78 (2001) 781–783.
[7] T. Saha-Dasgupta, D.D. Sarma, Phys. Rev. B. 64 (2001) 064408-6.
[8] D. Stoeffler, S. Colis, J. Magn. Magn. Mater. 290 (2005) 400–404.
[9] D. Niebieskikwiat, R.D. Sánchez, A. Caneiro, L. Morales, M. Vásquez-Mansilla, F. Rivadulla, L.E. Hueso, Phys. Rev. B 62 (2000) 3340–3345.
[10] O. Chmaissem, R. Kruk, B. Dabrowski, D.E. Brown, X. Xiong, S. Kolesnik, J.D. Jorgensen, C.W. Kimball, Phys. Rev. B. 62 (2000) 14197–14206.
[11] B. Martínez, J. Navarro, L. Balcells, J. Fontcuberta, J. Phys., Condens. Matter 12 (2000) 10515–10521.
[12] J. Navarro, C. Frontera, Ll. Balcells, B. Martínez, J. Fontcuberta, Phys. Rev. B 64 (2001) 092411–092414.
[13] D. Serrate, J.M. De Teresa, J. Blasco, M.R. Ibarra, L. Morellón, Appl. Phys. Lett. 80 (2002) 4573–4575.
[14] X.M. Feng, G.H. Rao, G.Y. Liu, W.F. Liu, Z.W. Ouyang, J.K. Liang, Solid State Commun. 129 (2004) 753–755.
[15] K.I. Kobayashi, T. Kimura, T. Tomioka, H. Sawada, K. Terakura, Phys. Rev. B 59 (1999) 11159–11162.
[16] Z. Fang, K. Terakura, J. Kanamori, Phys. Rev. B 63 (2001) 180407-4.
[17] M. Retuerto, M.J. Martínez-Lope, M. García-Hernández, J.A. Alonso, Mater. Res. Bull. 44 (2009) 1261–1264.
[18] G.M. Veith, M. Greenblatt, M. Croft, J.B. Goodenough, Mater. Res. Bull. 36 (2001) 1521–1530.
[19] M.J. Martínez-Lope, M.T. Casais, J.A. Alonso, Z. Naturforsch. 61b (2006) 164–169.
[20] M.T. Weller, S.J. Skinner, Int. J. Inorg. Mater. 2 (2000) 463–467.
[21] D. Armytage, B.E.F. Fender, Acta Crystallogr. B30 (1974) 809–812.
[22] R. Marchand, R. Pastuszak, Y. Laurent, G. Roult, Rev. Chim. Min. 19 (1982) 684–689.
[23] N. Diot, R. Marchand, J. Haines, J.M. Léger, P. Macaudière, S. Hull, J. Solid State Chem. 146 (1999) 390–393.
[24] M. Yang, J. Oró-Solé, J.A. Rodgers, A.B. Jorge, A. Fuertes, J.P. Attfield, Nat. Chem. 3 (2011) 47–52.
[25] H.M. Rietveld, J. Appl. Crystallogr. 2 (1969) 65–71.
[26] T. Roisnel, J. Rodriguez-Carvajal, Mater. Sci. Forum 378-381 (2001) 118–123.
[27] J. Rodríguez-Carvajal, T. Roisnel, Int. Union Crystallogr. Newsletter No 20 (1998).
[28] J. Rodríguez-Carvajal, Physica B 192 (1993) 55–69.
[29] P. Thompson, D.E. Cox, J.B. Hastings, J. Appl. Crystallogr. 20 (1987) 79–83.
[30] B. van Laar, W.B. Yelon, Appl. Crystallogr. 17 (1984) 47–54.
[31] L.W. Finger, D.E. Cox, A.P. Jephcoat, Appl. Crystallogr. 27 (1994) 892–900.
[32] R.A. Brand, Nucl. Instrum., Methods Phys. Rev. B 28 (1987) 398.
[33] R. Marchand, Y. Laurent, J. Guyader, P. L'Haridon, P. Verdier, J. Eur. Ceram. Soc. 8 (1991) 197–213.
[34] S.H. Elder, F.J. DiSalvo, L. Topor, A. Navrotsky, Chem. Mater. 5 (1993) 1545–1553.
[35] S.J. Clarke, K.A. Harstone, C.W. Michie, M.J. Rosseinsky, Chem. Mater. 14 (2002) 2664–2669.
[36] R.D. Shannon, Acta Crystallogr. A32 (1976) 751–767.
[37] D. Logvinovich, H.M. Agirre, J. Hejtmanek, R. Aguiar, S.G. Ebbinghaus, A. Reller, A.J. Weidenkaff, Sol. State Chem. 181 (2008) 2243–2249.
[38] M. Retuerto, M.J. Martínez-Lope, M. García-Hernández, J.A. Alonso, J. Phys.: Condens. Matter 21 (2009) 186003.
[39] R. Mishra, O.D. Restrepo, P.M. Woodward, W. Windl, Chem. Mater. 22 (2010) 6092.